# Chapter 1
# Quantum Fluids of Exciton-Polaritons and Ultracold Atoms

**Michiel Wouters**

**Abstract** We give an overview of the physics of quantum degenerate Bose gases of ultracold atoms and of exciton polaritons in microcavities. The physical systems are described and the main experimentally accessible observables are outlined. We give a schematic overview of recent trends in both fields.

## 1.1 Introduction

The physics of the quantum Bose gases took off from the theoretical side, when Einstein predicted that the bosonic statistics induces a phase transition in a noninteracting gas at low temperatures, when the interparticle distance is comparable to the de Broglie wave length [39]. Below the transition temperature, the gas enters the Bose-Einstein (BE) condensed phase, where a macroscopic number of particles occupies the lowest momentum state, leading to the coherence of the phase over macroscopic distances. The first physical example of this type of transition was superfluid Helium. Due to the strong interactions between the Helium atoms however, its theoretical description is complicate and the connection to the ideal Bose gas is not so direct. Still the macroscopic phase coherence and superfluidity are not qualitatively altered by the strength of interactions, so that the ideal Bose gas remains conceptually a good starting point to understand the remarkable behavior of superfluid Helium. It was in this context that Bogoliubov analyzed the effect of weak interactions and Pitaevskii constructed the classical theory for inhomogeneous Bose-Einstein condensates.

A physical realization of the weakly interacting Bose gas was lacking for many years. The condition of weak interactions $nR_e^3 \ll 1$ is only satisfied when the interparticle distance ($n^{-1/3}$) is much larger than the range of the interactions ($R_e$). No gases satisfy this condition at thermodynamic equilibrium. Several ideas were pursued to create metastable quantum gases that are in the weakly interacting limit. Both excitons in semiconductors and very dilute atomic gases were conceived to

M. Wouters (✉)
TQC, Universiteit Antwerpen, Universiteitsplein 1, 2610 Antwerpen, Belgium
e-mail: michiel.wouters@ua.ac.be

A. Bramati, M. Modugno (eds.), *Physics of Quantum Fluids*,
Springer Series in Solid-State Sciences 177, DOI 10.1007/978-3-642-37569-9_1,

be good candidates to achieve this goal. The first successful realization was obtained with dilute atoms in 1995 [13]. The condensation of excitons on the other hand proved to be much harder due to the complicated solid state environment. By coupling the exciton to a cavity photon, polariton quasi-particles are created. Because of their much lighter mass as compared to the exciton, they are much easier to condense in the ground state. Unambiguous proof hereof was obtained in 2006 [28].

The ultracold dilute atomic gases have turned out a very flexible system, and can be used as emulators for a wide variety of quantum systems and the field has witnessed a vigorous expansion. It is beyond the scope of the present introduction to cover this field. We will rather restrict ourselves to the physics of bosonic atoms in the regime of weak interactions. On the polariton side, the relative simplicity of the experiments has allowed for many milestone experiments to be performed in a relatively short time. The field being still much smaller than the cold atom one, we will cover relatively more of the polariton physics.

## 1.2 The Systems

In the following sections, we will start with short separate introductions to the microcavity and cold atom systems to describe their specific features.

### *1.2.1 The Microcavity Polariton System*

#### 1.2.1.1 Microcavity Polariton Properties

A microcavity is a solid state Fabri-Perrot cavity with a distance between the mirrors of the order of one micron. The mirrors are flat so that the photon modes have a conserved momentum in the directions parallel to the mirror plane, making them a two-dimensional (2D) system. At small momenta, their dispersion is in good approximation quadratic $\omega_C(k) = \omega_C^0 + k^2/2m_C$, where the effective mass is four orders of magnitude smaller than the free electron mass $m_C = 10^{-4}m_e$. The resonance frequency $\omega_C^0$ is in the electron volt range, the typical energy scale of electronic transitions. The mirrors are usually Distributed Bragg reflectors (DBRs) with a quality factor of the order of 10.000, yielding photon line widths in the 0.1 meV range, corresponding to a few ps life time [15].

When a material is placed between the mirrors, that has an electronic transition in resonance with the optical mode, the electronic excitations couple to the light. Of particular interest is the coupling to an excitonic transition (bound electron hole pair) in the material, illustrated in Fig. 1.1(a). When a photon creates an exciton, the center of mass momentum of the exciton is equal to the photon momentum. The relative wave function of the exciton being fixed, the coupling between a photon and exciton at momentum $\mathbf{k}$ can be seen as the coupling in a two-level system. In

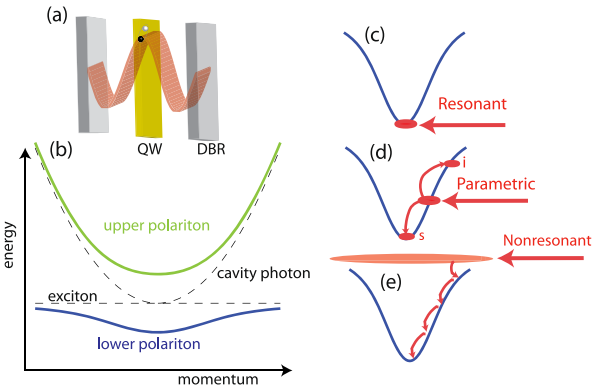


**Fig. 1.1** (**a**) Overview of the microcavity polariton system. A cavity photon is strongly coupled to an exciton transition in an embedded quantum well. (**b**) The dispersion of the upper (*green*) and lower (*blue*) polaritons, compared to the bare exciton and photon dispersions (*dashed lines*). (**c**), (**d**), (**e**) comparison of the different excitation schemes: resonant (**c**), parametric (**d**) and nonresonant (**e**)

second quantization, this coupling can be described by a term in the Hamiltonian of the form

$$H_R = \frac{\Omega_R}{2} \sum_{\mathbf{k}} \psi_C^\dagger(\mathbf{k}) \psi_X(\mathbf{k}) + h.c. \tag{1.1}$$

where the coupling parameter $\Omega_R$ is the Rabi frequency and $\psi_C$ annihilates a cavity photon. The operator $\psi_C$ describes the annihilation of an exciton (electron-hole pair). To enhance the binding energy, the exciton is usually confined in a quantum well. The eigenstates of the full linear Hamiltonian $H = H_0 + H_R$, with the free Hamiltonian

$$H_0 = \sum_{\mathbf{k}} \left[ \omega_C(k)\, \psi_C^\dagger(\mathbf{k}) \psi_C(\mathbf{k}) + \epsilon_X\, \psi_X^\dagger(\mathbf{k}) \psi_X(\mathbf{k}) \right], \tag{1.2}$$

can be obtained by diagonalizing it at fixed $\mathbf{k}$. The dispersion of the quasi-particles, the so-called lower and upper polaritons, is shown in Fig. 1.1(b). The splitting between upper and lower polariton was first experimentally seen by Weisbuch et al. in 1992 [56]. Note that in (1.2), we have neglected the momentum dependence of the exciton energy, which is well justified since its mass is around four orders of magnitude heavier than the cavity photon.

The coupling between excitons and photons is determined by the Rabi frequency $\Omega_R$, that is of the order of a few meV in GaAs up to 50 meV in GaN (discussed in Chap. 10), 130 meV in ZnO (see Chap. 11) and even higher in organic materials [1]. A larger Rabi frequency makes the polaritons more robust with respect to temperature. Experiments with GaAs microcavities are conducted at cryogenic temperatures around 10 K, where polaritons in GaN (see Chap. 10) and organic materials can be observed at room temperature. Many experiments are however conducted with GaAs microcavities, because the growth technology for this material is much

more advanced thanks to its use in commercial opto-electronic applications. Much progress has however been made in the fabrication of GaN microcavities and many of the pioneering experiments on polariton condensation have been conducted on a CdTe microcavity [28, 33, 42].

The microcavities are structurally identical to Vertical Cavity Surface Emitting Lasers (VCSELs). The only difference is that their excitonic resonance is carefully tuned to the cavity photon. The most important consequence hereof is that unlike photons, the polaritons interact significantly with each other. Indeed, the excitons consist of electrons and holes and their (exchange dominated) interaction is responsible for the polariton-polariton interactions [11]. It is theoretically modeled by adding the interaction term

$$H_I = \frac{g}{2}\int d\mathbf{x}\, \psi_X^\dagger(\mathbf{x})\psi_X^\dagger(\mathbf{x})\psi_X(\mathbf{x})\psi_X(\mathbf{x}) \tag{1.3}$$

to the Hamiltonian. Its approximation by a contact interaction is well justified, because the range of the exciton-exciton interaction potential is of the order of 10 nm, where the polariton physics takes place on the μm length scale.

On resonance, the polariton is half exciton and half photon, so that the effective polariton-polariton interaction is $g_{LP} = g/4$. The relevant dimensionless coupling constant that characterizes the strength of interactions in a 2D gas of particles with mass $m$ is $\tilde{g} = mg/\hbar^2$ [7]. This means that even though the excitons are in a regime of strong interactions $\tilde{g} = m_X g/\hbar^2 \sim 1$, the polaritons are in a weakly interacting regime. For example in GaAs microcavities, the dimensionless interaction constant is of the order of $\tilde{g} = m_{LP} g/\hbar^2 \approx 0.01$.

A second major difference with the bare exciton gas concerns the role of disorder. A certain degree of disorder due to growth fluctuations is inevitable. Fluctuations in the quantum well width result in an inhomogeneous effective potential for the excitons, with a correlation length on the nm scale and gives a inhomogeneous linewidth in the order of one meV. It however turns out that when the Rabi frequency is larger than this inhomogeneous broadening, the polariton modes are quite insensitive to the excitonic disorder [45]. The major source of disorder acting on the polaritons comes from the fluctuation in the distance between the two DBR mirrors. A monolayer fluctuation gives an energy shift of the order of 0.5 meV, which is of the same order of magnitude as the other polariton energy scales.

Controllable manipulation of the potential acting on the polaritons is possible by a variety of techniques, that are discussed in Chap. 8. Among the most successful strategies of creating potentials acting on the polaritons are etching (see Chaps. 8 and 9), stress induced traps [4], surface acoustic waves [10] and controlled variation of the DBR thickness (see Chap. 6).

So far, we have simplified the discussion by neglecting the polarization degree of freedom of the polaritons [47]. The photon however has two polarization states. In GaAs for example, there are four exciton polarization states. The photon only couples to the $m_z = \pm 1$ excitons. The other two states with $m_z = \pm 2$ are not coupled to the light because of angular momentum conservation. They are dark and do not form polaritons.

The single particle polariton eigenstates have a well defined linear polarization due to the splitting of both the photon and exciton linear polarization states. For what concerns the polariton-polariton interactions however, the conservation of angular momentum in collisions results in the conservation of the circularly polarized states. The interactions turn out to be anisotropic: the interactions between cocircular polarized polaritons is larger than between countercircularly polarized ones: $g_{\uparrow\uparrow} \gg |g_{\uparrow\downarrow}|$. This is due to the fact that the dominant contribution comes from the Pauli exclusion principle (exchange interaction). For countercircularly polarized excitons, both electron and hole spins are however different, so that the exchange contribution vanishes. The interactions due to higher order terms have been found to be negative $g_{\uparrow\downarrow} < 0$ [31, 54].

Discussions on the spin physics of polaritons can be found in Chaps. 3 and 4.

#### 1.2.1.2 Experiments with Polaritons

In its ground state, the microcavity is empty. Polaritons can be injected by means of optical or electrical injection. The polariton life time is mainly limited by the finite photon life time. In state of the art microcavities, it is around 10 ps, which is of the order of the other time scales of their dynamics and thus presents a severe limitation. Therefore, polaritons are often continuously injected in order to compensate for these losses. Two different optical injection schemes should be distinguished. The first excitation scheme is *resonant* excitation (see Fig. 1.1(c)): A laser is tuned to the polariton frequency at a given wave vector. The second scheme is *nonresonant* excitation (see Fig. 1.1(e)). In this latter case, the laser is tuned to an energy above the polariton energy. High energy excitons or free electron-hole pairs are formed, that subsequently relax to the bottom of the lower polariton branch. Electrical excitation has a similar effect.

An important difference between the resonant and nonresonant excitation schemes concerns the $U(1)$ phase symmetry of the polariton field. In the case of resonant excitation, the coupling of the external laser amplitude $F_L$ to the microcavity adds a term to the Hamiltonian

$$H_L = F_L e^{-i\omega_L t}\Psi^\dagger(\mathbf{k}_L) + h.c. \tag{1.4}$$

that explicitly breaks the $U(1)$ symmetry. The phase of the polariton field is determined by the phase of the laser and in particular its spatial and temporal coherence is determined by the coherence properties of the laser light. Under nonresonant excitation on the other hand, the $U(1)$ symmetry is not explicitly broken and polariton coherence can spontaneously form. Various models to describe this symmetry broken nonequilibrium state are discussed in Chap. 2.

An excitation scheme that is intermediate between resonant and nonresonant excitation is the so-called parametric excitation [25, 51]. The lower polariton branch is excited resonantly at an energy above the ground state carefully chosen so that polaritons can scatter into the ground state (signal) and an excited state (idler) through a single collision. The parametric scheme is illustrated in Fig. 1.1(d). Where under

parametric excitation, the phase of the pumped mode is fixed by the laser, the signal phase is chosen spontaneously, because only the sum of signal and idler phases is fixed $\phi_s + \phi_i = 2\phi_p$. Therefore, the spontaneous formation of coherence is observed when the density of polaritons in the signal mode is increased.

Finally, under pulsed resonant excitation, the polariton phase is only fixed as long as the laser pulse excites the microcavity and is free to evolve afterwards. The main limitation of this scheme is, as we mentioned earlier, the finite polariton life time that makes the density drop on the same time scale as the other time scales that are involved in the dynamics.

### *1.2.2 The Cold Atom System*

Similar to polaritons, also the dilute clouds of ultracold alkali atoms are not in their ground state, which is the solid phase. The relaxation to a solid however needs three-body interactions, which are very slow at low densities and the gas phase is metastable with a life time that can be of the order of one minute. This is much longer than the time needed to reach thermal equilibrium and much longer than the typical time scales of the dynamics. It is therefore a good approximation to neglect the finite life time of the trapped atoms.

Since the realization of Bose-Einstein condensation, the field of ultracold atoms has witnessed an explosive growth. Nowadays, many experiments are performed on atoms of bosonic and fermionic [21] statistics, that can be combined with ions [61] and strongly coupled to light [8]. The scope of this chapter is limited to point out some aspects of the physics of ultracold bosonic gases. More extensive reviews of their properties can be found in several text books on the subject [38, 39]. Due to the three-body losses, the maximum density of the atoms is around $n = 10^{14}$ cm$^{-3}$. This means that the typical interatomic spacing is similar to the polariton spacing of around 1 micron. Quantum degeneracy is reached when the de Broglie wavelength reaches this value. Due to the much heavier atomic mass, the temperature requirement for the atoms is much more severe and of the order of 100 nK, eight orders of magnitude smaller than in the polariton case. Thanks to the excellent isolation of the atomic clouds from any environment, these ultralow temperatures can however be routinely achieved. While the BEC phase transition does not rely on the interactions between the atoms, the transition temperature is affected by atomic interactions (see Chap. 16).

Spin conservation laws in the collisions of atoms make that for several combinations of hyperfine states, the number of atoms in each state is conserved. Mixtures of a well defined number of atoms in each hyperfine state can thus be prepared, which allows to study atomic gases with tunable effective spin.

Interactions between ultracold atoms have a range that is of the order of 10 nm, much shorter than their spacing. The interaction can thus be well approximated by

a contact interaction, that reads in three dimensions (omitting technicalities concerning their regularization)

$$V(\mathbf{x}) = \frac{4\pi\hbar^2 a_{sc}}{m}\delta(\mathbf{r}), \tag{1.5}$$

where $a_{sc}$ is the scattering length, that is typically of the order of the range of the interactions. Making use of so-called Feshbach resonances, the scattering length can be tuned at will. Both positive and negative signs for the scattering length can be reached. In absolute value, it can be tuned from zero to values larger than the interparticle spacing. In the latter regime, the atomic gas enters a very controlled strongly interacting regime.

An alternative route to the regime of strong interactions in bosons is by using optical lattices. These are periodic potentials generated by standing laser fields. They allow to realize a tunable bosonic Hubbard model, where the dramatic effects of interactions between bosonic particles were first evidenced in the superfluid to Mott insulator phase transition [22].

Interactions can be meaningfully compared between 2D polariton gases and 2D atomic clouds. The latter can be created by applying a standing laser field that confines the cloud in one dimension only. In experiments on the 2D Bose gas, the interaction strength is tunable and takes values in the range $\tilde{g} = 10^{-2}$–$0.3$ [12, 24, 26]. As discussed above, Microcavity polariton in GaAs microcavities are in the lower values of this range.

The coupling of ultracold gases to cavity photons has been achieved as well, making for a systems that is at first sight strongly analogous to the microcavity one. For example, in Ref. [8], a BEC was placed inside an optical cavity, that was tuned to an electronic transition of the atoms, a situation very similar to the quantum well embedded in a microcavity. An important difference between the two cases is the dimensionality of the photon. Where it has in the semiconductor case the same dimensionality as the exciton, in the atomic case, the photon is zero-dimensional where the condensate is 3D. A second ingredient that causes an important difference, where the motion of the Ga and As atoms is negligible for the crystalline solid state materials, the atoms move while they interact with the light, leading to optomechanical effects [8].

## 1.3 Observables

### *1.3.1 Microcavities*

The measurement of the polariton state inside the microcavity is straightforward, thanks to the one-to-one correspondence between the microcavity polaritons and the light that is transmitted through the microcavity mirrors [46]. Using standard optical techniques, the polariton density can be measured in real space $n(\mathbf{x})$ or in

momentum space $n(\mathbf{k})$. Using a spectrometer, the energy spectrum is readily obtained, resulting in images of $n(\mathbf{x}, \omega)$ or $n(\mathbf{k}, \omega)$. When a streak camera is used, the time evolution of the density can be monitored with a ps resolution.

By interfering the light that is emitted at different positions, the spatial coherence $g^{(1)}(\mathbf{x}_1, \mathbf{x}_2) = \langle \psi^+(\mathbf{x}_1)\psi(\mathbf{x}_2)\rangle / \sqrt{n(\mathbf{x}_1)n(\mathbf{x}_2)}$ can be measured [28]. From the interferrograms, also the average phase difference between different regions in the condensate can be extracted. This has allowed to evidence the existence of quantized vortices in polariton condensates [32]. This interference technique to visualize vortices has been first used for atomic condensates by Inouye et al. [27].

It is important to point out that all the measurements of polariton gases are performed over times that are very long as compared to the polariton life time. For a steady state measurement, this means that actually a long time average is recorded. In practice, the cw experiments are performed with long pulses. A typical measurement takes a time that is long with respect to the pulse duration and thus averages over many realizations of the condensate. For the observation of vortices, this means that only an average phase profile is measured, that completely misses moving vortices. For pulsed experiments where the time evolution is followed, the measurements record the average over multiple realizations of the dynamics. Again, the particular trajectory of a single realization cannot be followed.

### *1.3.2 Ultracold Atoms*

The main observable of ultracold atoms is the density: the atomic (column) density can be imaged through its absorption of laser light. It has turned out that from the density, combined with an engineered evolution of the system before recording it, an enormous wealth of information can be derived. The clearcut observation of BEC in 1995 was a density measurement performed a certain time after the trap was switched off. The free expansion maps approximately the momentum to the distance and thus gives a good estimate of the momentum distribution. A further analysis shows that the mapping of distance to momentum is modified by the interactions during the early stages of the expansion. Note that in the polariton case, the momentum distribution is also obtained by a kind of free expansion of the emitted photons. There however, interactions are always negligible, because the propagation takes fully place outside of the microcavity, where photon-photon interactions are absent.

Also from the *in situ* measurements of the atomic clouds, important information can be extracted. By using high resolution optical [48] or scanning electron microscopy (SEM) techniques, the atomic density profiles can be measured with a resolution that is better than the interparticle distance and the lattice spacing of optical lattices. Thanks to the single atom sensitivity, also higher order correlations can be measured. This technique will be described in Chap. 18.

A crucial difference between the measurements of ultracold atoms and polaritons is that in the case of the ultracold atoms information is obtained from a single

shot measurement. A picture of a single realization of the ensemble of atoms is taken. This is relevant for phase measurements. Two atomic clouds can be made to interfere with each other and a particular realization of an experiment will always show interference fringes, irrespective of whether the phases of the two clouds are related or not. This makes it straightforward to observe spontaneous vortices [24]. The presence of a vortex is signaled by a fork like dislocation in the interference pattern between the condensate and a reference condensate. By repeating such an experiment many times, the probability distribution for the number of vortices can be measured.

Spectral information on the Bose gases can be extracted by applying time-dependent laser fields. An example is Bragg spectroscopy [50]. In this type of experiments, two lasers with frequency difference $\Delta\omega$ and wave vector difference $\Delta k$ are applied to the gas. A large response of the atoms is observed when $(\Delta k, \Delta\omega)$ coincides with a resonance in the structure factor. Another example is modulation spectroscopy, where the standing laser field that creates an optical lattice is modulated [52]. The excitation frequency and spectrum turns out to be a precise probe for the properties of the quantum fluid.

For the measurement of temporal coherence, Ramsey type experiments can be used. A proposal for the measurement of the temporal coherence of atomic condensates is discussed in Chap. 15.

## 1.4 Physical Properties

### *1.4.1 Condensate Shape*

In contrast to conventional condensed matter systems such as the electron gas or superfluid Helium, both the ultracold atoms and polariton gases are strongly inhomogeneous. The overall trapping potential acting on cold atoms is usually well approximated by a quadratic potential. In the polariton case, not only trapping potentials can be present, but also the excitation that injects particles is inhomogeneous. The physical consequences of the inhomogeneity are very different for systems at thermodynamic equilibrium and for nonequilibrium gases.

In the case of cold atoms in equilibrium, the effect of a shallow quadratic trapping potential can in good approximation be described in the local density approximation. This means that the gas can be treated locally as homogeneous at a given chemical potential $\mu(\mathbf{r})$. This chemical potential varies in space as $\mu(\mathbf{r}) = \mu_0 - V_{ext}(\mathbf{r})$, where $V_{ext}$ is the trapping potential. What at first sight could seem to be a complication, actually turns out to be a convenience: one has access to a range of chemical potentials in a single experiment. Measuring the local density, it is possible to extract the equation of state $\mu(n)$, from which thermodynamic quantities such as the pressure and phase space density can be extracted. A discussion on this method in the context of the unitary Fermi gas is given in Chap. 17.

In the polariton case on the other hand, the inhomogeneity induces more complicated phenomena. Due to the nonequilibrium situation, that breaks time reversal symmetry, the steady state can sustain flows of polaritons. In other terms, the superfluid phase is not guaranteed to be homogeneous in the steady state. For a general inhomogeneous potential $V_{ext}(\mathbf{r})$ and inhomogeneous injection of particles $P(\mathbf{r})$, it is not possible to find a steady state with a uniform superfluid phase. Because of these flows, it is a much harder problem to find the steady state. It has been observed that when exciting the polariton gas with a very small pump spot, the condensation mainly takes place at a finite wave vector. The physical interpretation is that most of the particles are flowing away from the region where they are created [42, 57]. It is even possible that under certain conditions, these flows appear under the form of quantized vortices [32]. Thanks to the polarization degree of freedom, even more complex topological structures such as half vortices can be generated [34].

## *1.4.2 Coherence*

### 1.4.2.1 Spatial Coherence

The order parameter of the Bose-Einstein condensation phase transition is the long range phase coherence, which means that for large separation $|\mathbf{x}_1 - \mathbf{x}_2| \to \infty$, the first order coherence goes to a nonzero condensate density $\langle \psi^\dagger(\mathbf{x}_1)\psi(\mathbf{x}_2)\rangle = n_c \neq 0$. In ultracold atomic gases, the nonzero value of the condensate density in a 3D condensate was observed experimentally in Ref. [6].

For one and two dimensional systems at finite temperature, the Hohenberg-Mermin-Wagner theorem asserts that no true long range order can exist, $n_c = 0$. In two dimensions, there is still a phase transition from a normal gas at high temperatures to a superfluid phase at low temperatures, that is of the Berezinskii-Kosterlitz-Thouless (BKT) type. Above the transition temperature, the phase coherence decays exponentially $\langle \psi^\dagger(\mathbf{x}_1)\psi(\mathbf{x}_2)\rangle \sim \exp(-|\mathbf{x}_1 - \mathbf{x}_2|/\ell_c)$. Moreover, above the transition temperature, one expects to see the spontaneous formation of vortices. Below the transition temperature, the coherence decays as a power law of the distance $\langle \psi^\dagger(\mathbf{x}_1)\psi(\mathbf{x}_2)\rangle \sim 1/|\mathbf{x}_1 - \mathbf{x}_2|^{\alpha(T)}$. For $T \to 0$, the power goes to zero as well and long range order is recovered at zero temperature. In a finite size system, the gas can already show coherence over its full extent at finite temperature.

Pancake shaped clouds of bosonic atoms have been used to study the Kosterlitz-Thouless transition experimentally. The spontaneous vortices were observed and the transition in the analytic behavior of the coherence was observed when the gas was cooled through the transition. The most difficult aspect of the cold atom experiments is the finite size of the system. The BKT transition is theoretically usually studied for homogeneous systems, but the finite size effects can mask the algebraic decay of long range order [23].

As we have pointed out in the general description of polariton quantum fluids, Sect. 1.2.1.2, only in nonresonantly and parametrically excited microcavities, there

is a spontaneous formation of coherence. Due to the nonequilibrium character where the steady state is determined as a balance between driving and dissipation, the phase fluctuations of the polariton condensates are much less understood.

A fundamental question concerns how the nonequilibrium situation affects the long range decay of the coherence. Theoretical calculations based on very different formalisms predict that in the limit of slow phase decay, the coherence still falls off algebraically in 2D [53] and exponentially in 1D [59]. While this behavior is the same as the equilibrium Bose gas at finite temperature, the exponent (2D) and coherence length (1D) are now determined by the strength of the losses rather than by the temperature. Moreover, the details of the coupling to the reservoir affect the coherence [60].

Clear experimental results on the spatial decay of the coherence are not available yet, mainly because the size of the polariton gas is still limited and because in many experiments disorder is too large. In the recent experiments by Spano et al. [49] on a high quality sample, the coherence length of a parametrically excited polariton condensate, the spatial coherence was found to extend over the whole condensate, without any sign of algebraic decay.

#### 1.4.2.2 Temporal Coherence

The coherence of a Bose gas does not only decay as a function of spatial distance, but also as a function of the time delay $t_1 - t_2$. For polariton condensates, the temporal coherence is in principle directly available from the spectrally resolved images

$$n(x,\omega) = \frac{1}{T}\int_0^T dt_1 dt_2 e^{i\omega(t_2-t_1)}\left\langle \psi^\dagger(\mathbf{x},t_1)\psi(\mathbf{x},t_2)\right\rangle. \tag{1.6}$$

The line narrowing at the threshold for condensation/parametric oscillation illustrates the expected increase in coherence time a mode gets macroscopically occupied. The same phenomenon takes place above the threshold of a normal laser.

Let us discuss briefly the main mechanisms that limit the coherence time of a laser. Far above the threshold, the temporal coherence of a laser is limited by the Shawlow-Townes phase diffusion, that predicts an exponential decay of the coherence with a decay time $\tau_{ST}^{-1} = 4N/\gamma$, where $\gamma$ is the bare cavity line width and $N$ the number of photons. The losses and gain contribute both equally to the magnitude of the decay rate. When the gain medium not only provides a gain for the photons, but also changes the refractive index and hence the cavity frequency, an additional contribution to the linewidth appears, the so-called Henry linewidth enhancement $\tau_H = \alpha^2\gamma/N$, where $\alpha = d\omega_C/dR$ is the ratio of the change in cavity frequency to the change in optical gain.

Both the Shawlow-Townes and Henry mechanisms are present in polariton condensates as well. In addition, the coherence time of polariton condensates is also limited by the polariton-polariton interactions [58].

For the case of atomic Bose-Einstein condensates, when losses are neglected, the only mechanism for phase decoherence comes from the interactions between

the atoms. The analysis by Castin and Sinatra, presented in Chap. 15, shows that the ensemble (microcanonical, canonical, grand canonical) changes the functional behavior of the temporal coherence.

### *1.4.3 Superfluidity*

The phase coherence of a Bose-Einstein condensed gas has profound consequences on its hydrodynamic behavior and shows effects such as persistent flows and quantization of vorticity. It has turned out that the phenomena associated to superfluidity are robust with respect to particle losses so that many of the phenomena that were first studied with $^4$He and ultracold atoms can also be observed in polariton gases.

A major consequence of Bose-Einstein condensation on an interacting system is the change in the spectrum of elementary excitations from quadratic to linear. According to the argument by Landau, this change of the excitation spectrum is responsible for the dissipationless flow of the superfluid component, because the energy cannot be lowered by creating excitations on top of the superfluid, at least for superfluid velocities below the speed of sound. When the speed of sound is exceeded, excitations are created and the superflow is dissipated.

The use of an energetic argument could suggest that the dissipationless flow is limited to systems at thermodynamic equilibrium, but this turns out not to be the case. The Landau critical velocity can be derived without relying on energetic minimization arguments. Let us limit ourselves to the case of static defects. The excitation spectrum on top of a moving condensate (in equilibrium or not) is obtained in the rest frame of the defect by a Galilean transformation. A static defect can only create excitations at the frequency of the condensate. As long as the condensate speed is below the speed of sound, no excitations can be created.

In the polariton case, this mechanism results in a strong suppression of the Rayleigh scattering when the polariton gas is in the superfluid regime. Since it is for this physics not important whether the superfluid phase coherence is spontaneous or not, the easiest experiment to observe the reduced scattering is under resonant excitation. Following the suggestion by Carusotto and Ciuti [9], this suppression was experimentally observed by Amo et al. [2], where a resonantly excited polariton condensate was collided with a natural defect on the sample. In the atomic condensate case, the experiments probing the dissipation of superfluidity were performed soon after the realization of BEC. The defect they used was created by a laser field that exerts a repulsive potential on the atoms [41].

The Landau argument being based on the linear excitation spectrum is only valid for weak perturbations that do not strongly change the condensate density and speed. For strong defects, the theoretical analysis by Frisch et al. [20] has shown that the critical velocity is lower by a factor of more than two. The physical reason is that a large defect strongly alters the density and speed of the superfluid. This implies that locally the Landau criterion can be violated when the asymptotic speed is still below the sound speed. In this case, the dissipation of the superflow does not take place

in the form of elementary phonon excitations, but rather in the periodic shedding of vortices (at lower speeds) or in the creation of a dark soliton (at higher speeds). Experimentally, both in cold atoms [37] and in polariton condensates [3, 36] (see Chaps. 6 and 7), this instability of the superflow was observed. An extensive discussion of the theory of the critical speed in atomic condensates is given in Chap. 12.

The quantization of vorticity is a key feature of superfluids. Soon after the realization of Bose Einstein condensation of ultracold atoms, quantized vortices and vortex lattices were generated by rotating the trap. The study of rotating atomic gases have allowed for a detailed study of many phenomena of rotating Bose gases, such as the Kelvin modes of vortex lines and the Tkachenko modes of vortex lattices [18]. Currently, there is a great interest in reaching the regime of ultrafast rotation where correlated quantum hall states can be created. One of the most promising techniques are artificial gauge fields created by a properly designed laser field [14].

Furthermore, when many vortices are present they can form complex tangles, a quantum turbulent state. The theory of quantum turbulence applied to ultracold atomic gases is discussed in Chap. 13, where pioneering experiments are discussed in Chap. 14.

In polariton condensates, mechanical rotation speeds needed to induce vortices are technically not achievable, but in this case the nonequilibrium situation can lead to the spontaneous formation of vortices [32] and even the formation of vortex lattices has been predicted [29].

The interplay between the polarization degree of freedom and superflows gives rise to the existence of topological defects that are more complicate than standard quantized vortices. These objects are discussed in Chaps. 4 and 5.

### *1.4.4 Disorder*

The effect of disorder on quantum systems has proven to be very rich. The original studies were motivated by the unavoidable presence of random fluctuations when solid state structures are fabricated. The problem of a particle moving in a random potential whose magnitude is described by a statistical distribution has become an important field of research. Already on the level of single particle physics, random potentials have a dramatic impact on the behavior of quantum systems. The solutions of the wave equation are qualitatively different. As it was shown by Anderson, waves are always localized in a 1D random potential, where in 3D, there is a mobility edge, i.e. an energy above which the waves can propagate through the whole space.

In the case of ultracold atomic gases, potential fluctuations are absent, but this makes the atomic gases an almost ideal testing bed for the precise study of the effect of disorder on quantum systems, by applying an additional laser field with random intensity distribution [44]. The polariton system is rather in a standard solid state situation, where the disorder is unavoidable and often of the same order as the other energy scales.

In the cold atom gases, the Anderson localization of waves in a 1D random potential was clearly demonstrated by several groups. The disorder is made by applying a laser beam on the atoms whose intensity varies randomly in space. In the presence of such a random potential, the atoms can no longer propagate, but the density distribution at long times shows an exponential decay, characteristic for the Anderson localized states [5, 43].

When interactions enter into play, the physical picture becomes much richer. On the one hand the interactions screen out the disorder potential and thus delocalize the Bose gas, on the other hand the interactions cause dephasing that is detrimental to superfluidity. The ground state of the strictly noninteracting Bose gas is the state where all the particles are in the lowest energy state, that is exponentially localized. These exponentially localized states below to the so-called Lifshitz tail. In the thermodynamic limit where the number of particles goes to infinity, the density goes to infinity as well. An infinitesimal amount of interactions dramatically changes the ground state, that spreads over many of the low-lying localized states and forms many islands, a 'fragmented' state.

When the interaction strength is increased, the density spreads out and starts to cover space more and more homogeneously. Consequently, the coherence of the Bose gas improves. On the mean field level, the defragmentation transition coincides with the Bose glass to superfluid transition, where the spatial coherence decay goes from exponential to algebraic. Interactions can thus enhance the coherence of a disordered Bose gas. This trend is opposite to the quantum depletion of a homogeneous condensate that grows with the interaction strength. This effect of quantum fluctuations starts to dominate when the mean field theory breaks down, i.e. in the case of strong interactions when the interaction energy is of the order of the tunneling energy to go from one to the next valey in the disorder potential. The disorder potential then amplifies the effect of quantum fluctuations due to interactions in a way that is similar to a periodic potential, where the celebrated superfluid to Mott insulator phase occurs. At a critical strength of the disorder potential, a phase transition to the Bose glass phase occurs, that is in analogy with the Mott insulator phase not superfluid. The difference between the Mott insulator and Bose glass phases is that the excitation spectrum that is gapped in the Mott insulator and not gapped in the Bose glass phase [19].

### *1.4.5 Dynamics*

An advantage of both the atom and polariton systems is that the time scales of their dynamics are slower than the temporal resolution of the measurements. This allows to study the temporal dynamics of the observables. Moreover, the external forces acting on the systems can be varied fast with respect to the dynamics.

For cold atoms, the collective excitations that are excited when the clouds are shaken have revealed a wealth of information on their properties. For example, the frequency of the breathing mode gives information on the equation of state, where

the scissor mode is very sensitive to the superfluidity of the gas [39]. Typically, the oscillation amplitude is moderate and the oscillation frequencies can be computed in linear response theory.

A more recent direction of the field concerns the study of dynamics far from equilibrium. For a review, we refer to Ref. [40]. One of the pioneering experiments on the dynamics far from equilibrium was performed in 2006 by Kinoshita et al. They created a one-dimensional Bose gas, that is a close experimental realization of the Lieb-Liniger gas. The atoms were put in a superposition of the momentum states $\pm p_0$ and it was observed that the momentum distribution remained non-Gaussian, even after thousands of collisions. This lack of thermalization was interpreted in terms of the integrability of the Lieb-Liniger gas. This experiment motivated a great body of theoretical studies on questions concerning ergodicity and integrability [40].

A second field of interest concerns quantum quenches. Here a control parameter is changed so that the system undergoes a phase transition. For classical phase transitions, this is typically the temperature; for quantum phase transitions it is rather the coupling constant that tunes the system through the quantum critical point. It is then predicted that excitations will be created through the so-called Kibble-Zurek (KZ) mechanism [30, 62]. In the case of Bose-Einstein condensation, those excitations are quantized vortices and they were observed experimentally by Weiler et al. [55]. In these experiments, the temperature was quickly lowered below the critical one and the spontaneously formed vortices were observed. Related experiments were performed with exciton-polaritons [35], where the density was suddenly increased above the critical density. The subsequent buildup of the spatial coherence was monitored, but no spontaneous vortices were observed, because so far no experimental technique exists to visualize them (see Sect. 1.3.1).

With respect to dynamics, we remind that the polariton system is intrinsically in a non-equilibrium situation when the driving compensates for the losses. One has to resort do descriptions of the dynamics to assess the properties of the stationary state. In most cases, the steady state of the ultracold atomic gases corresponds to a thermal state that can be described with statistical methods. The flexibility of ultracold atoms has however also generated proposals to study driven-dissipative dynamics with ultracold atoms, where an environment is engineered so to introduce nonequilibrium phase transitions [16] and topological states of matter [17].

## References

1. V.M. Agranovich, *Excitations in Organic Solids*. International Series of Monographs on Physics (Oxford University Press, London, 2009)
2. A. Amo, J. Lefrere, S. Pigeon, C. Adrados, C. Ciuti, I. Carusotto, R. Houdre, E. Giacobino, A. Bramati, Superfluidity of polaritons in semiconductor microcavities. Nat. Phys. **5**(11), 805–810 (2009)
3. A. Amo, S. Pigeon, D. Sanvitto, V.G. Sala, R. Hivet, I. Carusotto, F. Pisanello, G. Lemenager, R. Houdre, E. Giacobino, C. Ciuti, A. Bramati, Hydrodynamic solitons in polariton superfluids. Science **332**, 1167–1170 (2011)

4. R. Balili, V. Hartwell, D. Snoke, L. Pfeiffer, K. West, Bose-Einstein condensation of microcavity polaritons in a trap. Science **316**(5827), 1007–1010 (2007)
5. J. Billy, V. Josse, Z. Zuo, A. Bernard, B. Hambrecht, P. Lugan, D. Clement, L. Sanchez-Palencia, P. Bouyer, A. Aspect, Direct observation of Anderson localization of matter waves in a controlled disorder. Nature **453**(7197), 891–894 (2008)
6. I. Bloch, T.W. Hansch, T. Esslinger, Measurement of the spatial coherence of a trapped Bose gas at the phase transition. Nature **403**(6766), 166–170 (2000)
7. I. Bloch, J. Dalibard, W. Zwerger, Many-body physics with ultracold gases. Rev. Mod. Phys. **80**, 885–964 (2008)
8. F. Brennecke, T. Donner, S. Ritter, T. Bourdel, M. Kohl, T. Esslinger, Cavity QED with a Bose-Einstein condensate. Nature **450**(7167), 268–271 (2007)
9. I. Carusotto, C. Ciuti, Probing microcavity polariton superfluidity through resonant Rayleigh scattering. Phys. Rev. Lett. **93**, 166401 (2004)
10. E.A. Cerda-Méndez, D.N. Krizhanovskii, M. Wouters, R. Bradley, K. Biermann, K. Guda, R. Hey, P.V. Santos, D. Sarkar, M.S. Skolnick, Polariton condensation in dynamic acoustic lattices. Phys. Rev. Lett. **105**, 116402 (2010)
11. C. Ciuti, V. Savona, C. Piermarocchi, A. Quattropani, P. Schwendimann, Role of the exchange of carriers in elastic exciton-exciton scattering in quantum wells. Phys. Rev. B **58**, 7926–7933 (1998)
12. P. Cladé, C. Ryu, A. Ramanathan, K. Helmerson, W.D. Phillips, Observation of a 2D Bose gas: From thermal to quasicondensate to superfluid. Phys. Rev. Lett. **102**, 170401 (2009)
13. F. Dalfovo, S. Giorgini, L.P. Pitaevskii, S. Stringari, Theory of Bose-Einstein condensation in trapped gases. Rev. Mod. Phys. **71**, 463–512 (1999)
14. J. Dalibard, F. Gerbier, G. Juzeliūnas, P. Öhberg, Colloquium: Artificial gauge potentials for neutral atoms. Rev. Mod. Phys. **83**, 1523–1543 (2011)
15. B. Deveaud, *The Physics of Semiconductor Microcavities* (Wiley, New York, 2007)
16. S. Diehl, A. Micheli, A. Kantian, B. Kraus, H.P. Buchler, P. Zoller, Quantum states and phases in driven open quantum systems with cold atoms. Nat. Phys. **4**(11), 878–883 (2008)
17. S. Diehl, E. Rico, M.A. Baranov, P. Zoller, Topology by dissipation in atomic quantum wires. Nat. Phys. **7**(12), 971–977 (2011)
18. A.L. Fetter, Rotating trapped Bose-Einstein condensates. Rev. Mod. Phys. **81**(2), 647–691 (2009)
19. M.P.A. Fisher, P.B. Weichman, G. Grinstein, D.S. Fisher, Boson localization and the superfluid-insulator transition. Phys. Rev. B **40**, 546–570 (1989)
20. T. Frisch, Y. Pomeau, S. Rica, Transition to dissipation in a model of superflow. Phys. Rev. Lett. **69**, 1644–1647 (1992)
21. S. Giorgini, L.P. Pitaevskii, S. Stringari, Theory of ultracold atomic Fermi gases. Rev. Mod. Phys. **80**, 1215–1274 (2008)
22. M. Greiner, O. Mandel, T. Esslinger, T.W. Hansch, I. Bloch, Quantum phase transition from a superfluid to a Mott insulator in a gas of ultracold atoms. Nature **415**(6867), 39–44 (2002)
23. Z. Hadzibabic, J. Dalibard, Two-dimensional Bose fluids: An atomic physics perspective, in *Nano Optics and Atomics: Transport of Light and Matter Waves*, Proceedings of the International School of Physics "Enrico Fermi", vol. CLXXIII, ed. by D. Wiersma, R. Kaiser, L. Fallani (2011)
24. Z. Hadzibabic, P. Krueger, M. Cheneau, B. Battelier, J. Dalibard, Berezinskii–Kosterlitz–Thouless crossover in a trapped atomic gas. Nature **441**, 1118 (2006)
25. R. Houdré, C. Weisbuch, R.P. Stanley, U. Oesterle, M. Ilegems, Nonlinear emission of semiconductor microcavities in the strong coupling regime. Phys. Rev. Lett. **85**, 2793–2796 (2000)
26. C.-L. Hung, X. Zhang, N. Gemelke, C. Chin, Observation of scale invariance and universality in two-dimensional Bose gases. Nature **470**(7333), 236–239 (2011)
27. S. Inouye, S. Gupta, T. Rosenband, A.P. Chikkatur, A. Görlitz, T.L. Gustavson, A.E. Leanhardt, D.E. Pritchard, W. Ketterle, Observation of vortex phase singularities in Bose-Einstein condensates. Phys. Rev. Lett. **87**, 080402 (2001)

28. J. Kasprzak, M. Richard, S. Kundermann, A. Baas, P. Jeambrun, J.M.J. Keeling, F.M. Marchetti, M.H. Szymanska, R. Andre, J.L. Staehli, V. Savona, P.B. Littlewood, B. Deveaud, L.S. Dang, Bose-Einstein condensation of exciton polaritons. Nature **443**(7110), 409–414 (2006)
29. J. Keeling, N.G. Berloff, Spontaneous rotating vortex lattices in a pumped decaying condensate. Phys. Rev. Lett. **100**(25), 250401 (2008)
30. T.W.B. Kibble, Topology of cosmic domains and strings. J. Phys. A, Math. Gen. **9**(8), 1387 (1976)
31. D.N. Krizhanovskii, S.S. Gavrilov, A.P.D. Love, D. Sanvitto, N.A. Gippius, S.G. Tikhodeev, V.D. Kulakovskii, D.M. Whittaker, M.S. Skolnick, J.S. Roberts, Self-organization of multiple polariton-polariton scattering in semiconductor microcavities. Phys. Rev. B, Condens. Matter Mater. Phys. **77**(11), 115336 (2008)
32. K.G. Lagoudakis, M. Wouters, M. Richard, A. Baas, I. Carusotto, R. Andre, L.S. Dang, B. Deveaud-Pledran, Quantized vortices in an exciton-polariton condensate. Nat. Phys. **4**(9), 706–710 (2008)
33. K.G. Lagoudakis, T. Ostatnický, A.V. Kavokin, Y.G. Rubo, R. André, B. Deveaud-Plédran, Observation of half-quantum vortices in an exciton-polariton condensate. Science **326**(5955), 974–976 (2009)
34. K.G. Lagoudakis, T. Ostatnicky, A.V. Kavokin, Y.G. Rubo, R. Andre, B. Deveaud-Pledran, Observation of half-quantum vortices in an exciton-polariton condensate. Science **326**(5955), 974–976 (2009)
35. G. Nardin, K.G. Lagoudakis, M. Wouters, M. Richard, A. Baas, R. André, L.S. Dang, B. Pięţka, B. Deveaud-Plédran, Dynamics of long-range ordering in an exciton-polariton condensate. Phys. Rev. Lett. **103**, 256402 (2009)
36. G. Nardin, G. Grosso, Y. Leger, B. Pięţka, F. Morier-Genoud, B. Deveaud-Pledran, Hydrodynamic nucleation of quantized vortex pairs in a polariton quantum fluid. Nat. Phys. **7**(8), 635–641 (2011)
37. T.W. Neely, E.C. Samson, A.S. Bradley, M.J. Davis, B.P. Anderson, Observation of vortex dipoles in an oblate Bose-Einstein condensate. Phys. Rev. Lett. **104**, 160401 (2010)
38. C. Pethick, H. Smith, *Bose-Einstein Condensation in Dilute Gases* (Cambridge University Press, Cambridge, 2002)
39. L. Pitaevskii, S. Stringari, *Bose-Einstein Condensation* (Oxford University Press, London, 2003)
40. A. Polkovnikov, K. Sengupta, A. Silva, M.V. Colloquium, Nonequilibrium dynamics of closed interacting quantum systems. Rev. Mod. Phys. **83**, 863–883 (2011)
41. C. Raman, M. Köhl, R. Onofrio, D.S. Durfee, C.E. Kuklewicz, Z. Hadzibabic, W. Ketterle, Evidence for a critical velocity in a Bose-Einstein condensed gas. Phys. Rev. Lett. **83**, 2502–2505 (1999)
42. M. Richard, J. Kasprzak, R. Romestain, R. André, L.S. Dang, Spontaneous coherent phase transition of polaritons in CdTe microcavities. Phys. Rev. Lett. **94**, 187401 (2005)
43. G. Roati, C. D'Errico, L. Fallani, M. Fattori, C. Fort, M. Zaccanti, G. Modugno, M. Modugno, M. Inguscio, Anderson localization of a non-interacting Bose-Einstein condensate. Nature **453**(7197), 895–898 (2008)
44. L. Sanchez-Palencia, M. Lewenstein, Disordered quantum gases under control. Nat. Phys. **6**(2), 87–95 (2010)
45. V. Savona, Effect of interface disorder on quantum well excitons and microcavity polaritons. J. Phys. Condens. Matter **19**(29), (2007)
46. V. Savona, C. Piermarocchi, A. Quattropani, P. Schwendimann, F. Tassone, Optical properties of microcavity polaritons. Phase Transit. **68**(1, Part B), 169–279 (1999)
47. I.A. Shelykh, A.V. Kavokin, Y.G. Rubo, T.C.H. Liew, G. Malpuech, Polariton polarization-sensitive phenomena in planar semiconductor microcavities. Semicond. Sci. Technol. **25**(1), 013001 (2010)
48. J.F. Sherson, C. Weitenberg, M. Endres, M. Cheneau, I. Bloch, S. Kuhr, Single-atom-resolved fluorescence imaging of an atomic Mott insulator. Nature **467**(7311), 68–72 (2010)

49. R. Spano, J. Cuadra, C. Lingg, D. Sanvitto, M.D. Martin, P.R. Eastham, M. van der Poel, J.M. Hvam, L. Vina, Build up of off-diagonal long-range order in microcavity exciton-polaritons across the parametric threshold (2011). arXiv:1111.4894
50. J. Stenger, S. Inouye, A.P. Chikkatur, D.M. Stamper-Kurn, D.E. Pritchard, W. Ketterle, Bragg spectroscopy of a Bose-Einstein condensate. Phys. Rev. Lett. **82**, 4569–4573 (1999)
51. R.M. Stevenson, V.N. Astratov, M.S. Skolnick, D.M. Whittaker, M. Emam-Ismail, A.I. Tartakovskii, P.G. Savvidis, J.J. Baumberg, J.S. Roberts, Continuous wave observation of massive polariton redistribution by stimulated scattering in semiconductor microcavities. Phys. Rev. Lett. **85**(17), 3680–3683 (2000)
52. T. Stöferle, H. Moritz, C. Schori, M. Köhl, T. Esslinger, Transition from a strongly interacting 1D superfluid to a Mott insulator. Phys. Rev. Lett. **92**, 130403 (2004)
53. M.H. Szymanska, J. Keeling, P.B. Littlewood, Nonequilibrium quantum condensation in an incoherently pumped dissipative system. Phys. Rev. Lett. **96**(23), 230602 (2006)
54. M. Vladimirova, S. Cronenberger, D. Scalbert, K.V. Kavokin, A. Miard, A. Lemaître, J. Bloch, D. Solnyshkov, G. Malpuech, A.V. Kavokin, Polariton-polariton interaction constants in microcavities. Phys. Rev. B **82**, 075301 (2010)
55. C.N. Weiler, T.W. Neely, D.R. Scherer, A.S. Bradley, M.J. Davis, B.P. Anderson, Spontaneous vortices in the formation of Bose-Einstein condensates. Nature **455**(7215), 948–951 (2008)
56. C. Weisbuch, M. Nishioka, A. Ishikawa, Y. Arakawa, Observation of the coupled exciton-photon mode splitting in a semiconductor quantum microcavity. Phys. Rev. Lett. **69**, 3314–3317 (1992)
57. E. Wertz, L. Ferrier, D.D. Solnyshkov, R. Johne, D. Sanvitto, A. Lemaitre, I. Sagnes, R. Grousson, A.V. Kavokin, P. Senellart, G. Malpuech, J. Bloch, Spontaneous formation and optical manipulation of extended polariton condensates. Nat. Phys. **6**(11), 860–864 (2010)
58. D.M. Whittaker, P.R. Eastham, Coherence properties of the microcavity polariton condensate. Europhys. Lett. **87**(2), 27002 (2009)
59. M. Wouters, I. Carusotto, Absence of long-range coherence in the parametric emission of photonic wires. Phys. Rev. B **74**, 245316 (2006)
60. M. Wouters, V. Savona, Stochastic classical field model for polariton condensates. Phys. Rev. B **79(16)**, 165302 (2009)
61. C. Zipkes, S. Palzer, C. Sias, M. Kohl, A trapped single ion inside a Bose-Einstein condensate. Nature **464**(7287), 388–391 (2010)
62. W.H. Zurek, Cosmological experiments in superfluid helium? Nature **317**(6037), 505–508 (1985)

http://www.springer.com/978-3-642-37568-2

Physics of Quantum Fluids
New Trends and Hot Topics in Atomic and Polariton Condensates
Bramati, A.; Modugno, M. (Eds.)
2013, XXII, 405 p., Hardcover
ISBN: 978-3-642-37568-2